SUPPLEMENTARY INFORMATION

Supplementary Method: Multiple particle tracking for size prediction with mixed particle sizes

Agarose gels were prepared using similar methods as above. However, two types of PS-COOH nanoparticles were added to each well instead of a single type of particle. For the 40/200nm experiment, 40nm PS-COOH nanoparticles (660/680, Fisher Scientific, Hampton, NH) and 200nm (505/515) were added to each well containing agarose gel and mixed until evenly distributed to achieve a concentration of 0.005% solids. For the 40/100nm experiment, 40nm PS-COOH nanoparticles (660/680, Fisher Scientific, Hampton, NH) and 100nm (505/515) were added to each well containing agarose gel and mixed until evenly distributed to achieve a concentration of 0.005% solids. Four samples were prepared for each combination. The prepared gels were allowed to set overnight at room temperature. Five videos were collected per particle type per well using light of wavelengths 640nm and 488nm to track the 40nm and 100/200nm particles, respectively.

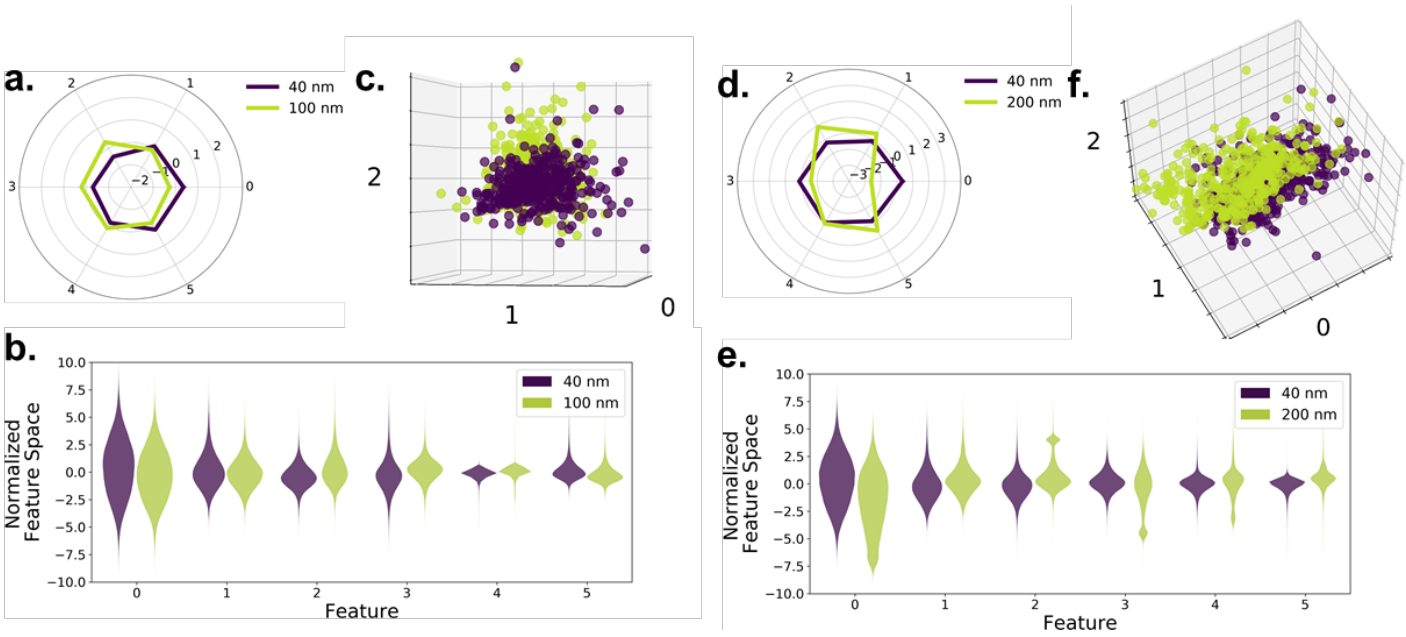

Figure S1. Size-dependent nanoparticle PCA analysis with mixed particle batches for 40/100nm PS-COOH and 40/200nm PS-COOH mixtures. (a., d.) Average component profile of PCA analysis stratified by particle size. (b., e.) Principle component distributions of PCA analysis stratified by particle size. (c., f.) The first three primary components of 400 randomly selected trajectories per size plotted against each other.

Figure S2

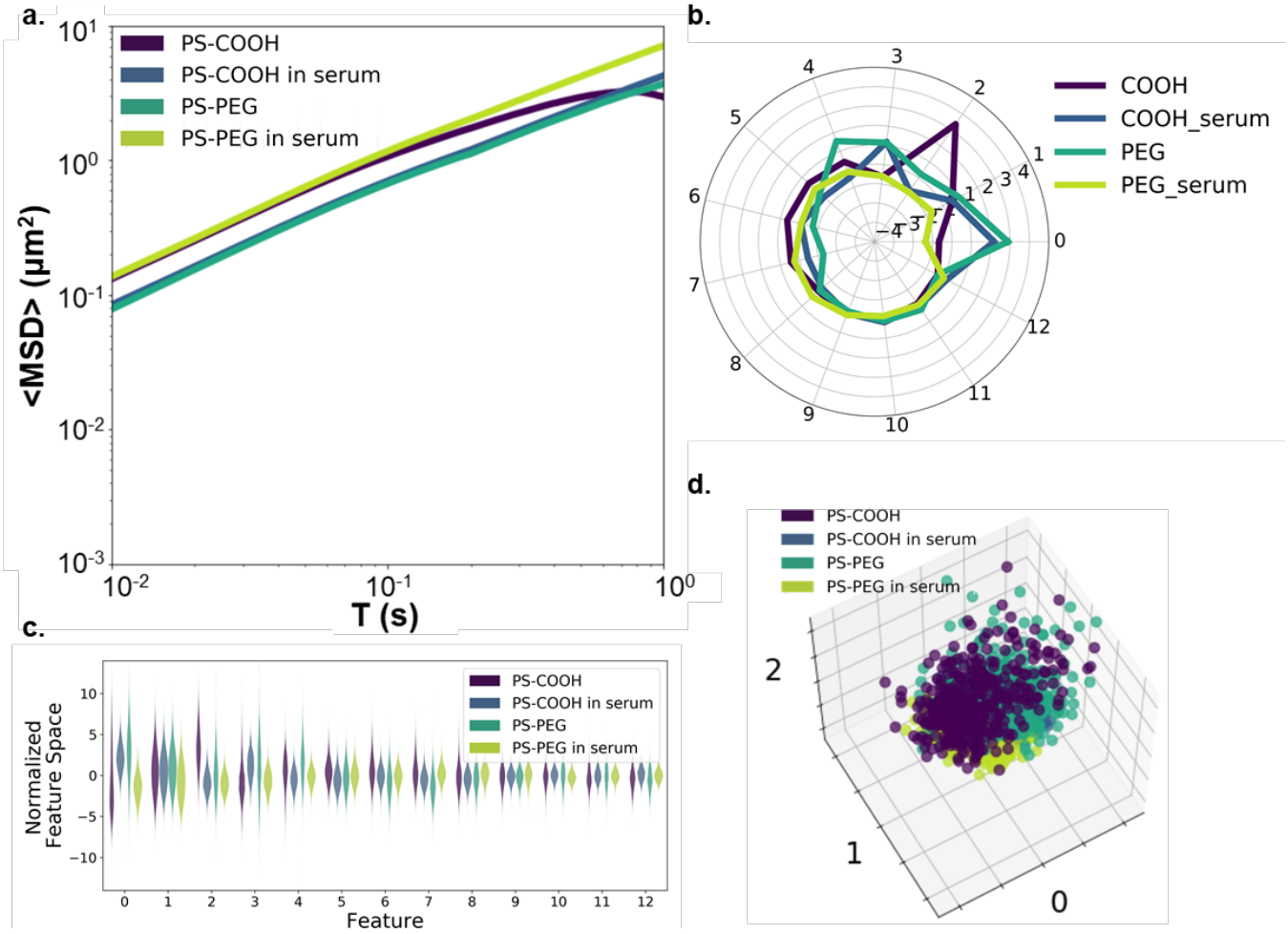

Figure S2. (a) Ensemble-averaged precision-weighted MSD profiles of 100-nm PS-COOH NPs, PS-PEG NPs, PS-COOH NPs incubated in horse serum, and PS-PEG NPs incubated in serum in 0.4% agarose gel (n=2 wells per particle type, n=5 videos per well). 95% confidence intervals (CIs) represented as semi-transparent shaded regions. (purple: PS-COOH, blue: PS-COOH in serum, teal: PS-PEG, yellow-green: PS-PEG in serum). (b) Average component profile of PCA analysis stratified by particle type. (c) Principle component distributions of PCA analysis stratified by particle type. (d) First three primary components of 400 randomly selected trajectories per particle type from entire trajectory dataset plotted against each other (purple: PS-COOH, blue: PS-COOH in serum, teal: PS-PEG, yellow-green: PS-PEG in serum).

Figure S3

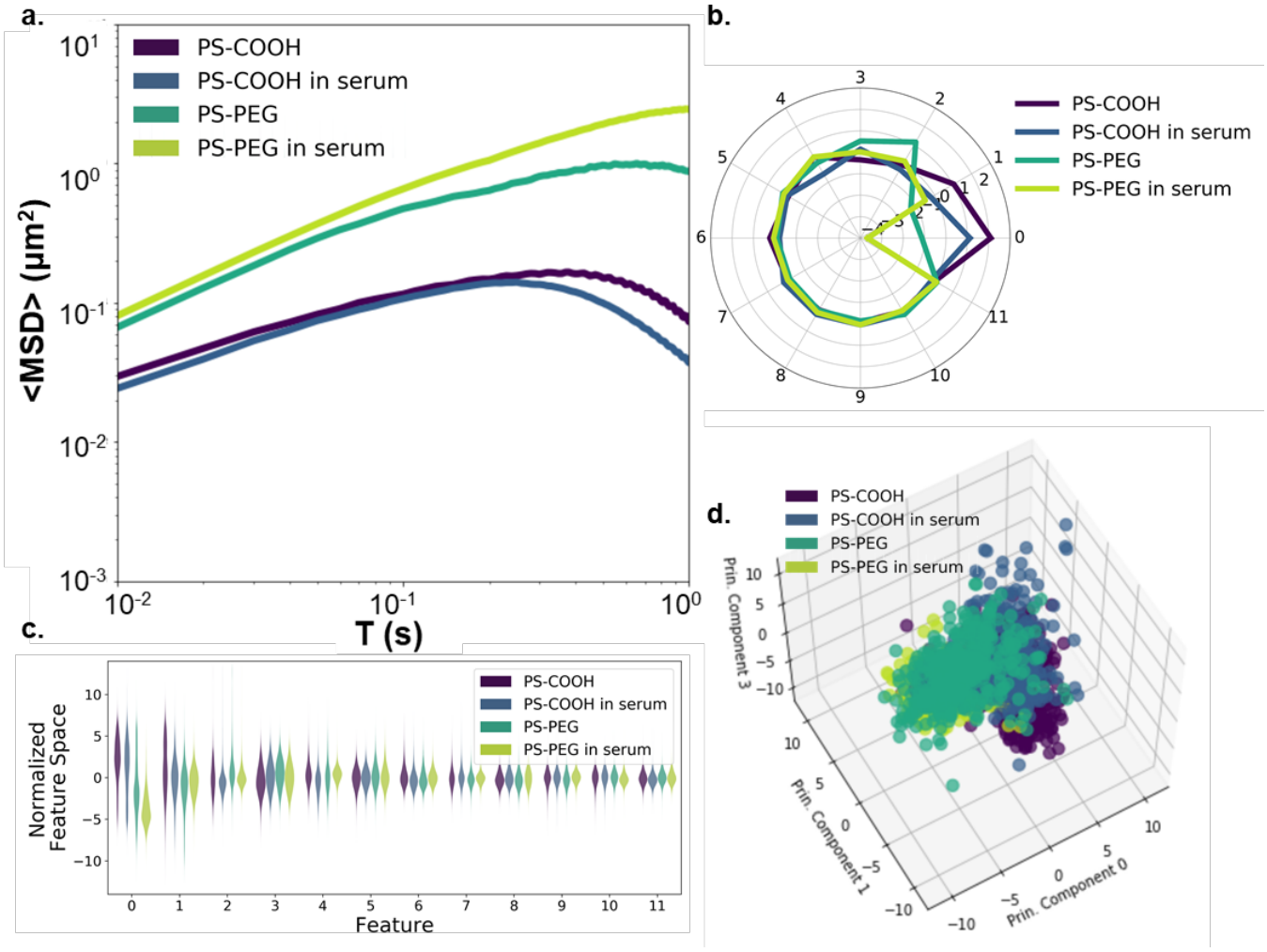

Figure S3. (a) Geometric ensemble-averaged precision-weighted MSD profiles of 100-nm PS-COOH NPs, PS-PEG NPs, PS-COOH NPs incubated in horse serum, and PS-PEG NPs incubated in serum in cortex of 300μm-thick rat brain slices (n=2 pups per particle type, n=2 slices per pup, 10 videos per slice). 95% confidence intervals (CIs) represented as semi-transparent shaded regions. (purple: PS-COOH, blue: PS-COOH in serum, teal: PS-PEG, yellow-green: PS-PEG in serum). (b) Average component profile of PCA analysis stratified by particle type. (c) Principle component distributions of PCA analysis stratified by particle type. (d) First three primary components of 400 randomly selected trajectories per particle type from entire trajectory dataset plotted against each other.

Figure S4

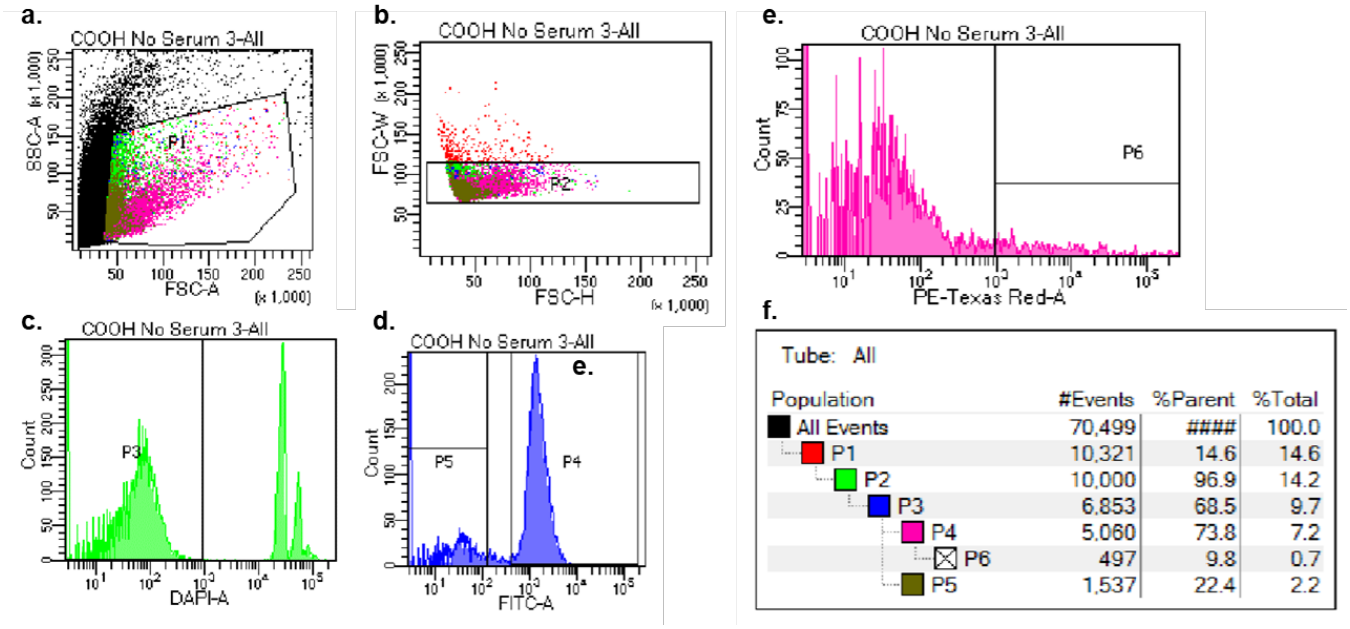

Figure S4. Example FACS analysis. (a) Polygonal forward-scatter side-scatter gate to filter out cell debris, (b) forward scatter-height and forward scatter-width gate to filter out cell doublets, (c) DAPI gate to filter out dead cells, (d) FITC gate to filter out non-microglial cells, (e) Texas Red threshold defining PS-positive cells, and (f) population map.

Figure S5

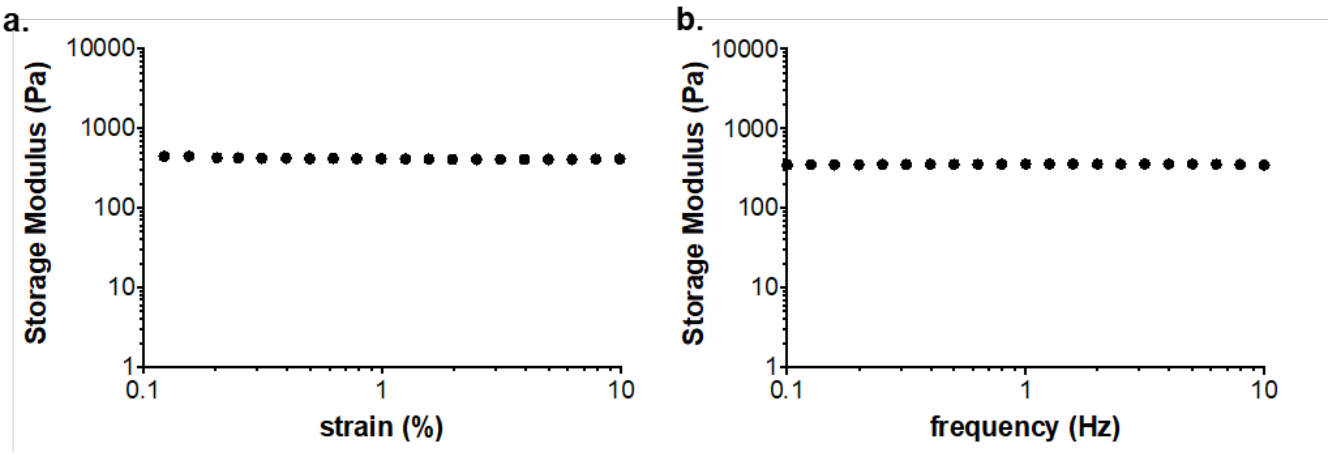

Figure S5. The linear viscoelastic region of 0.4% agarose was determined by performing a strain (a) and frequency (b) sweep following a 4 h incubation at 22°C. For the strain sweep, the frequency was fixed at 1 Hz, and the storage and loss moduli were measured at various strains (0.1 – 10%). For the frequency sweep, the strain was fixed at 2%, and the storage and loss moduli were measured at various frequencies (0.1 – 10 Hz). The sweeps demonstrate that at 2% strain and 2 Hz, the agarose gel is in the linear viscoelastic region because minor changes in strain or frequency do not change the measured storage modulus.

Figure S6

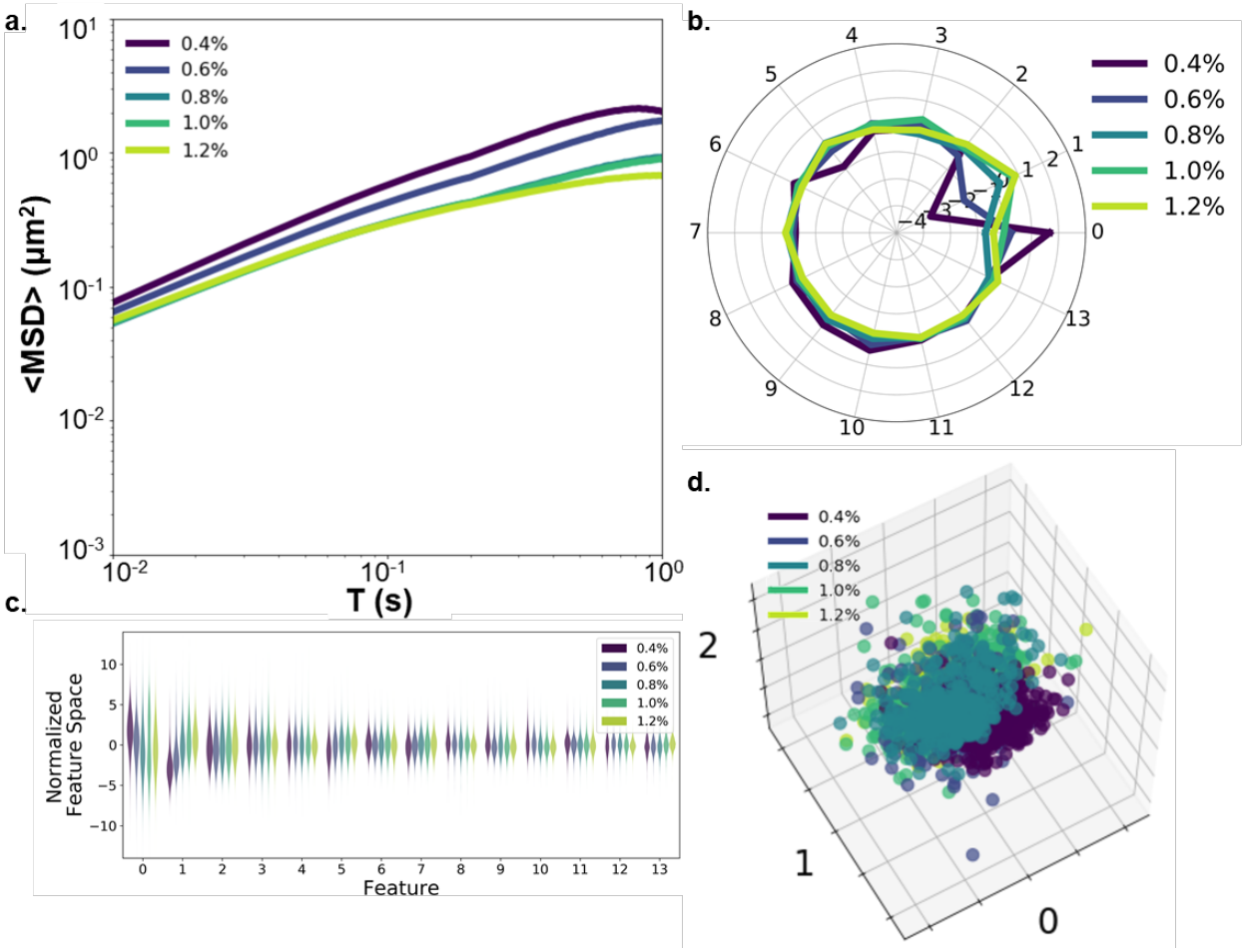

Figure S6. (a) Geometric ensemble-averaged precision-weighted MSD profiles of 100-nm PS-COOH NPs in 0.4%, 0.6%, 0.8%, 1.0%, and 1.2% agarose gels (n=2 wells per condition, n=5 videos per well). 95% confidence intervals (CIs) represented as semi-transparent shaded regions. (purple: 0.4%, blue: 0.6%, teal: 0.8%, light-green: 1.0%, yellow-green: 1.2%). (b) Average component profile of PCA analysis stratified by percent agarose. (c) Principle component distributions of PCA analysis stratified by percent agarose. (d) First three primary components of 400 randomly selected trajectories per size from entire trajectory dataset plotted against each other.

Figure S7

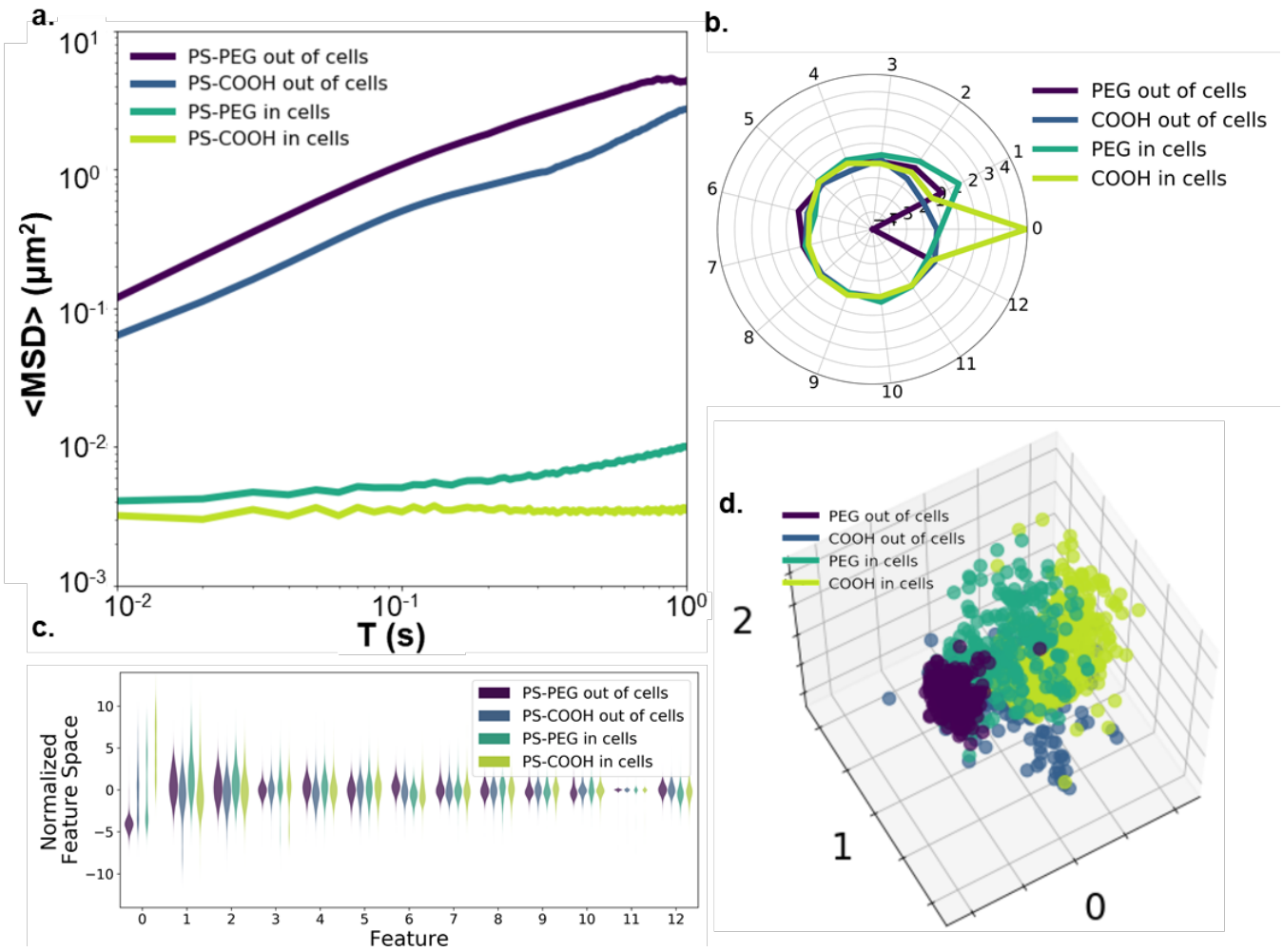

Figure S7. (a). Geometric ensemble-averaged precision-weighted <MSD> profiles of PS-COOH and PS-PEG NPs diffusing either intra- or extracellularly (n=2 wells per condition, 5 videos per well). 95% confidence intervals (CIs) represented as semi-transparent shaded regions. (purple: PS-PEG out of cells, blue: PS-COOH out of cells, teal: PS-PEG in cells, yellow-green: PS-COOH in cells). (b) Average component profile of PCA analysis stratified by particle type. (c) Principle component distributions of PCA analysis stratified by particle type. (d) First three primary components of 400 randomly selected trajectories per particle type from the entire trajectory dataset plotted against each other.

Table S1. Descriptions and calculations for each trajectory feature using trajectories from multiple particle tracking.

Feature	Description	How it is determined
alpha (α)	Exponent of the anomalous diffusion equation.	Non-linear least squares is used to fit raw MSD vs. lag time (τ) data to the anomalous diffusion equation: $MSD = 4D_{fit}\tau^{\alpha}$
Effective diffusion coefficient (D_{fit})	Coefficient of the anomalous diffusion equation.	Non-linear least squares is used to fit raw MSD vs. lag time (τ) data to the anomalous diffusion equation: $MSD = 4D_{fit}\tau^{\alpha}$
Kurtosis (K)	The fourth moment of the projected positions on the dominant eigenvector of the radius of gyration tensor (T).	$K = \frac{1}{N}\sum_{i=0}^{N-1}\frac{(x_i^p - \overline{x^p})^4}{\sigma_{x^p}^4}$
Asymmetry1 (a)	Characterizes the asymmetry of the trajectory. Asymmetry1 equals 0 for circularly symmetric trajectories and 1 for linear trajectories.	$a = \frac{(\lambda_1^2 - \lambda_2^2)^2}{(\lambda_1^2 + \lambda_2^2)^2}$, where λ_1 and λ_2 are the eigenvalues of radius of gyration tensor T: $\mathrm{T} = \begin{pmatrix} \frac{1}{N}\sum_{j=1}^{N}(x_j - \langle x\rangle)^2 & \frac{1}{N}\sum_{j=1}^{N}(x_j - \langle x\rangle)(y_j - \langle y\rangle) \\ \frac{1}{N}\sum_{j=1}^{N}(x_j - \langle x\rangle)(y_j - \langle y\rangle) & \frac{1}{N}\sum_{j=1}^{N}(y_j - \langle y\rangle)^2 \end{pmatrix}$
Asymmetry2 (a_2)	The ratio of the smaller to larger principal radius of gyration.	$a_2 = \frac{\lambda_2}{\lambda_1}$
Asymmetry3 (a_3)	An asymmetry feature that accounts for non-cylindrically symmetric point distributions.	$a_3 = -\log\left(1 - \frac{(\lambda_1 - \lambda_2)^2}{2(\lambda_1 + \lambda_2)^2}\right)$
Aspect ratio (AR)	The ratio of the long and short side of the trajectory's minimum bounding rectangle. Perfectly symmetric trajectories have an aspect ratio of 1, and aspect ratio increases as trajectories become more elongated	$AR = \begin{cases} \frac{\lvert x_{max} - x_{min}\rvert}{\lvert y_{max} - y_{min}\rvert}, & \lvert y_{max} - y_{min}\rvert < \lvert x_{max} - x_{min}\rvert \\ \frac{\lvert y_{max} - y_{min}\rvert}{\lvert x_{max} - x_{min}\rvert}, & \lvert y_{max} - y_{min}\rvert \geq \lvert x_{max} - x_{min}\rvert \end{cases}$
Elongation	An estimation of amount of extension of the trajectory from its centroid.	Elongation $= 1 - (\frac{1}{AR})$
Boundedness (B)	Boundedness quantifies how much a particle with diffusion coefficient D_{eff} is restricted by a circular confinement of radius r when diffusing for a period of time $N\Delta t$.	$B = \frac{D_{eff}N\Delta t}{r^2}$
Fractal Dimension (D_f)	Fractal dimension is a measure of how "complicated" a self similar figure is.	$D_f = \frac{\log(N)}{\log(NdL^{-1})}$
Trappedness (p_t)	The probability (p_t) that a particle with diffusion coefficient D_{eff} is trapped in a region (r_0) for a period of time $N\Delta t$.	$p_t = 1 - \exp(0.2048 - 0.25117(\frac{D_{eff}N\Delta t}{r_0^2}))$
Efficiency (E)	The ratio of squared net displacement to the sum of squared step lengths.	$E = \frac{(x_{N-1} - x_0)^2 + (y_{N-1} - y_0)^2}{\sum_{i=1}^{N-1}(x_i - x_{i-1})^2 + (y_i - y_{i-1})^2}$
Straightness (S)	The ratio of net displacement to the sum of step lengths.	$S = \frac{\sqrt{(x_{N-1} - x_0)^2 + (y_{N-1} - y_0)^2}}{\sum_{i=1}^{N}\sqrt{(x_i - x_{i-1})^2 + (y_i - y_{i-1})^2}}$
MSD Ratio (MSD_{n_1,n_2})	MSD ratio characterizes the shape of the MSD curve. For Brownian motion, it is 0; For restricted motion it is < 0; For directed motion it is > 0.	$MSD_{n_1,n_2} = \frac{MSD_{n_1}}{MSD_{n_2}} - \frac{n_1}{n_2}$
Frames	The total number of frames the trajectory spans.	Frames = N
D_{eff1}	Effective diffusion coefficient at 0.1 s.	$D_{eff1} = \frac{MSD_{\tau=0.1}}{4*0.1}$
D_{eff2}	Effective diffusion coefficient at 1 s.	$D_{eff2} = \frac{MSD_{\tau=1}}{4*1}$

MSD: mean squared displacement
N: number of frames
σ_{x^p}: standard deviation of the projected 2D positions
λ_1,λ_2: eigenvalues of radius of gyration tensor
D_{eff}: effective diffusion coefficient
r: radius of circular confinement
n: frame number
r_0: radius of trapped region
i_{Back}: average background pixel intensity
τ: lag time
x^p: projected 2D position
T: gyration tensor
$\langle x\rangle$,$\langle y\rangle$: average x and y location
Δt: inverse of frame rate
d: largest distance between any two positions
L: total length (sum over all steplengths) of trajectory
σ_I: standard deviation of pixel intensities

Table S2. Classifier metrics using nanoparticle trajectories to predict particle size in a mixture of 40/100 nm particles in 0.4% agarose gels (n=4 wells per mixture, n=5 videos per well).

	Sample Size		Stokes-Einstein		Stokes-Einstein[1]		Neural Network	
	Training	Test	Training	Test	Training	Test	Training	Test
40 nm	106482	108446	0.539	0.530	0.636	0.626	0.773	0.764
100 nm	106645	108571	0.782	0.780	0.674	0.699	0.655	0.664
Avg/Tot	**213127**	**217017**	**0.661**	**0.655**	**0.655**	**0.648**	**0.714**	**0.714**

[1] Predictions performed including an anomalous diffusion coefficient.

Table S3. Classifier metrics using nanoparticle trajectories to predict particle size in a mixture of 40/200nm particles in 0.4% agarose gels (n=4 wells per mixture, n=5 videos per well).

	Sample Size		Stokes-Einstein		Stokes-Einstein[1]		Neural Network	
	Training	Test	Training	Test	Training	Test	Training	Test
40 nm	24728	25022	0.732	0.729	0.797	0.793	0.877	0.858
200 nm	24589	25578	0.900	0.893	0.813	0.810	0.820	0.834
Avg/Tot	**49317**	**50600**	**0.816**	**0.811**	**0.805**	**0.802**	**0.848**	**0.846**

[1] Predictions performed including an anomalous diffusion coefficient.

Table S4 Classifier metrics using nanoparticle trajectories to predict particle type (PS-COOH, PS-COOH in serum, PS-PEG, and PS-PEG in serum) in organotypic rat brain slice model using a leave-one-out train-test split (n=2 pups, n=2 slices per pup).

	Neural Network[1,2]		Neural Network[1,3]		Neural Network[1,4]		Neural Network[1,5]	
	Training	Test	Training	Test	Training	Test	Training	Test
PS-COOH	0.786	0.210	0.776	0.533	0.696	0.735	0.760	0.506
PS-COOH in serum	0.849	0.706	0.832	0.714	0.791	0.634	0.866	0.330
PS-PEG	0.475	0.069	0.322	0.039	0.510	0.105	0.504	0.045
PS-PEG in serum	0.863	0.740	0.875	0.522	0.791	0.578	0.909	0.726
Avg/Tot	**0.743**	**0.431**	**0.701**	**0.452**	**0.697**	**0.513**	**0.756**	**0.402**

[1]Predictions performed using locally averaged features
[2]Predictions based on 3-1 slice train-test split using the first slice of four.
[3]Predictions based on 3-1 slice train-test split using the second slice of four.
[4]Predictions based on 3-1 slice train-test split using the third slice of four.
[5]Predictions based on 3-1 slice train-test split using the fourth slice of four.

Table S5. Classifier metrics using nanoparticle trajectories to predict particle type (PS-COOH, PS-COOH in serum) in organotypic rat brain slice model using a leave-one-out train-test split (n=2 pups, n=2 slices per pup).

	Neural Network[1,2]		Neural Network[1,3]		Neural Network[1,4]		Neural Network[1,5]	
	Training	Test	Training	Test	Training	Test	Training	Test
PS-COOH	0.824	0.307	0.820	0.567	0.794	0.709	0.892	0.567
PS-COOH in serum	0.928	0.814	0.893	0.734	0.869	0.702	0.927	0.393
Avg/Tot	**0.876**	**0.561**	**0.857**	**0.650**	**0.831**	**0.706**	**0.910**	**0.480**

[1]Predictions performed using locally averaged features
[2]Predictions based on 3-1 slice train-test split using the first slice of four.
[3]Predictions based on 3-1 slice train-test split using the second slice of four.
[4]Predictions based on 3-1 slice train-test split using the third slice of four.

[5]Predictions based on 3-1 slice train-test split using the fourth slice of four.

Table S6. Classifier metrics using nanoparticle trajectories to predict particle type (PS-PEG and PS-PEG in serum) in organotypic rat brain slice model using a leave-one-out train-test split (n=2 pups, n=2 slices per pup).

	Neural Network[1,2]		**Neural Network[1,3]**		**Neural Network[1,4]**		**Neural Network[1,5]**	
	Training	**Test**	**Training**	**Test**	**Training**	**Test**	**Training**	**Test**
PS-PEG	0.775	0.071	0.388	0.222	0.688	0.535	0.713	0.099
PS-PEG in serum	0.996	0.889	0.983	0.924	0.943	0.846	0.965	0.916
Avg/Tot	**0.870**	**0.479**	**0.684**	**0.573**	**0.815**	**0.690**	**0.839**	**0.508**

[1]Predictions performed using locally averaged features
[2]Predictions based on 3-1 slice train-test split using the first slice of four.
[3]Predictions based on 3-1 slice train-test split using the second slice of four.
[4]Predictions based on 3-1 slice train-test split using the third slice of four.
[5]Predictions based on 3-1 slice train-test split using the fourth slice of four.